Title

Rapid Estimation of Climate–Air Quality Interactions in Integrated Assessment Using a Response Surface Model

Journal

ACS Environmental Au, 3(3)

ISSN

2694-2518

Authors

Eastham, Sebastian D
Monier, Erwan
Rothenberg, Daniel
et al.

Publication Date

2023-05-17

DOI

10.1021/acsenvironau.2c00054

Peer reviewed

ACS ENVIRONMENTAL Au
AN OPEN ACCESS JOURNAL OF THE AMERICAN CHEMICAL SOCIETY

pubs.acs.org/environau Article

Rapid Estimation of Climate–Air Quality Interactions in Integrated Assessment Using a Response Surface Model

Sebastian D. Eastham,* Erwan Monier, Daniel Rothenberg, Sergey Paltsev, and Noelle E. Selin

Cite This: *ACS Environ. Au* 2023, 3, 153–163 Read Online

ACCESS | Metrics & More | Article Recommendations | Supporting Information

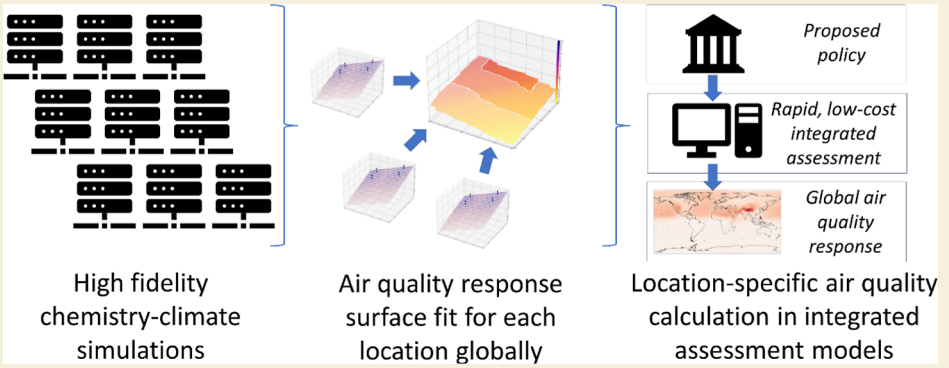

ABSTRACT: Air quality and climate change are substantial and linked sustainability challenges, and there is a need for improved tools to assess the implications of addressing these challenges together. Due to the high computational cost of accurately assessing these challenges, integrated assessment models (IAMs) used in policy development often use global- or regional-scale marginal response factors to calculate air quality impacts of climate scenarios. We bridge the gap between IAMs and high-fidelity simulation by developing a computationally efficient approach to quantify how combined climate and air quality interventions affect air quality outcomes, including capturing spatial heterogeneity and complex atmospheric chemistry. We fit individual response surfaces to high-fidelity model simulation output for 1525 locations worldwide under a variety of perturbation scenarios. Our approach captures known differences in atmospheric chemical regimes and can be straightforwardly implemented in IAMs, enabling researchers to rapidly estimate how air quality in different locations and related equity-based metrics will respond to large-scale changes in emission policy. We find that the sensitivity of air quality to climate change and air pollutant emission reductions differs in sign and magnitude by region, suggesting that calculations of "co-benefits" of climate policy that do not account for the existence of simultaneous air quality interventions can lead to inaccurate conclusions. Although reductions in global mean temperature are effective in improving air quality in many locations and sometimes yield compounding benefits, we show that the air quality impact of climate policy depends on air quality precursor emission stringency. Our approach can be extended to include results from higher-resolution modeling and also to incorporate other interventions toward sustainable development that interact with climate action and have spatially distributed equity dimensions.

KEYWORDS: *air quality, climate, integrated assessment, co-benefits, public health, global modeling*

1. INTRODUCTION

Air quality and climate are coupled problems but are still typically managed separately. Despite a need for coordination to design more effective policies, much previous research to inform climate and air quality actions has focused on assessing interventions primarily designed to achieve either climate or air quality targets, while treating the other as a side effect. Current modeling approaches are limited in their ability to simultaneously assess the implications of emission controls intended to reduce concentrations of harmful pollution and of climate policy that aims to reduce emissions of climate forcers such as greenhouse gases. Specifically, efforts to model the impacts of multiple intervention levers often sacrifice the detail needed to examine important distributional concerns. Here, we describe an approach that bridges the gap between integrated assessment modeling and full-scale atmospheric chemistry-climate simulations and illustrate its application to address the impact of different policy levers on population exposure to health-damaging pollutants such as ozone and fine particulate

Received: September 14, 2022
Revised: January 20, 2023
Accepted: January 20, 2023
Published: February 14, 2023

https://doi.org/10.1021/acsenvironau.2c00054
ACS Environ. Au 2023, 3, 153–163

matter ($PM_{2.5}$) in different global regions. Researchers have used different approaches to assess the implications of climate policy on air quality. Climate policy will have direct air quality consequences, which are often quantified as the "climate penalty" of greenhouse gas emissions.[1,2] Much research also focuses on the "co-benefits" of climate action, taking the climate action as primary and air quality and other impacts as secondary.[3,4] Recent work such as that by Hegwood et al.[5] has questioned the framing of such "co-benefits" as this implies a hierarchy of goals and priorities and does not reflect the growing importance of justice and equity in the climate debate.

Studies that are instead focused on the potential impact of air quality interventions often use models to simulate a single change while holding all other factors constant, including climate change.[6,7] This can support efforts to identify what sort of air quality control would yield the greatest contribution to achieving an air quality target but only as long as background conditions—including meteorology—remain approximately the same. Examples include estimating the contribution of individual power plants to US air pollution[8] or determining the air quality consequences of "excess" nitrogen oxide (NO_x) emissions from cars.[9] More generally, quantifications of the sensitivity of air quality to changes in different emissions can help to inform policy by indicating which interventions might be most effective.[10] There has also been work to assess how emission changes motivated by air quality concerns could affect the climate, such as the warming effect of removing sulfur from ship fuel.[11]

Recent work has argued for more coordinated climate and air quality efforts, recognizing both the presence of common sources and that the effect and effectiveness of emission regulation will evolve with a changing climate. Kinney[12,13] and von Schneidemesser et al.[14] have pointed out the need for more holistic consideration of air quality and climate policy. Some studies have used high-fidelity air quality models under different scenarios to directly compare the effects of air quality policy under different climate assumptions.[15−18] These studies show that greater air quality improvements are achievable through control of air pollutants than through avoidance of climate change in isolation, although factors such as the effect of temperature change on biogenic emissions (which can be ozone precursors) result in complex interactions. Other researchers have used integrated assessment models (IAMs) to provide rapid assessment of different scenarios, representing the effects of a broad slate of policy options on a range of relevant outcomes.[19−23] Although some IAMs focus on total economic impacts to inform quantities such as the Social Cost of Carbon (e.g., Nordhaus, 2014), others have been used specifically to show greater health benefits from "welfare-maximizing policies" rather than a pure focus on climate policy.[24]

Existing efforts to better understand how air quality and climate policy together might change environmental outcomes are currently limited by model capabilities and computational cost. Evaluating only specific scenarios in detailed models (which is necessary because of the high computational cost of each scenario) can potentially result in misleading estimates of the effects of a policy choice. Jafino et al.[25] discuss this in the context of adaptation policy, but the same is true when considering air quality policy. As an example, a future atmosphere might have greater marginal ozone production (per unit of NO_x emitted) than the current day, reflected in greater ozone production during pollution episodes.[26] This counterintuitively implies that air quality policy will become "more effective", even though the population's exposure to ozone would be greater in absolute terms under any proposed NO_x control policy than would be the case for the present day. Additional complications arise if baseline ozone concentrations have also been affected by climate change. In contrast, integrated assessment approaches inherently rely on simplified representations of key atmospheric and economic processes to remain computationally tractable and typically provide results at the scale of the global, regional, or national mean. However, the response of air quality to both climate and air quality policy is complex, with the same intervention (e.g., a decrease in NO_x emissions) sometimes having effects that vary in sign over the span of a few hundred kilometers. Regardless of the method used, focusing on global or regional mean responses can obscure the equity implications of climate and air quality policy.

Here, we describe an intermediate-fidelity approach that allows decision makers to understand and freely explore diverse scenarios of climate and air policy intervention—including their effects on equitability of outcomes—while minimizing the loss in accuracy. This "intermediate fidelity" approach lies at the intersection between low-fidelity approaches, such as a single regional estimate for the sensitivity of ozone to NO_x and climate change, and high-fidelity approaches such as expensive single-scenario chemistry-climate simulations. We do this by bridging between existing IAMs and chemistry-climate modeling. We use a full-complexity atmospheric chemistry-transport model that can accurately represent local chemical regimes to simulate global air quality under carefully chosen climate and air pollutant emission scenarios (see Methods), designed to explore the parameter space of plausible interventions. By fitting a response surface to the results for each location across Earth, we produce a rapid assessment model that can estimate the effect of simultaneous changes in air pollutants and climate on air quality. Although such approaches have been used previously in modeling of air quality impacts alone,[27] they have not to date been developed for climate−air quality interactions. This can facilitate assessment of multiple interventions that aim to reduce the health impact of air pollution. It also allows equity outcomes to be considered since the response is independently characterized in each individual location rather than using a global or regional mean. We then apply this approach to explore the challenge of achieving air quality goals under combined climate and air quality policy.

We first quantify the relationship between conventional air quality-relevant pollutants and outcomes, comparing our results to the existing literature. We then use the same data set to describe how interacting policies (specifically, those designed to control climate and air quality, respectively) could affect our ability to achieve air quality targets in the future.

2. METHODS

We perform a series of atmospheric chemistry simulations to project air quality under different climate and pollutant emission scenarios[28] in the late 21st century. Using a global atmospheric chemistry model, we simulate air quality under two different climate scenarios (corresponding to 3.7 and 10 W/m^2 in 2100), using five different realizations (ensemble members), and including perturbations to emissions of NO_x, SO_x, volatile organic compounds (VOCs), and ammonia (five cases, including the baseline).

From these 50 simulations, we fit response surfaces in every surface grid point with non-zero population, resulting in simplified models

https://doi.org/10.1021/acsenvironau.2c00054
ACS Environ. Au 2023, 3, 153−163

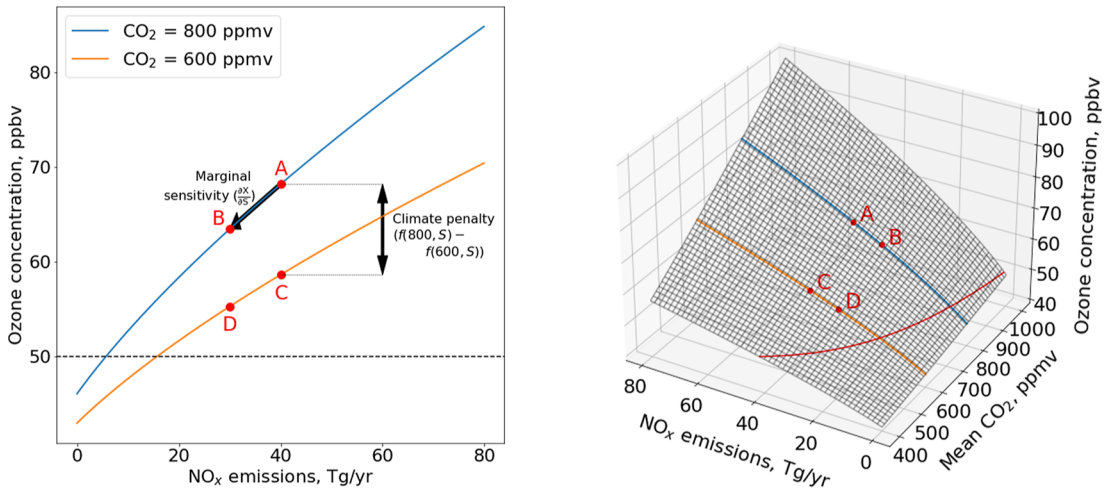

Figure 1. Response of surface air quality in one location to changes in air quality and climate policy. Left panel: typical representation of how air quality policy (NO_x emission stringency) might affect local air quality (ozone concentration) under two different climate policies (CO_2 levels). Right: demonstration of how the two lines in the left panel are actually curves on the surface of a more general response surface, where a surface ozone response can be defined for any combination of climate and air quality policy. The red points in the right-hand figure correspond to the results from individual simulations that can be used to develop a reduced-order estimate (e.g., a response plane—see Figure 2) of the response surface.

that allow us to evaluate the reductions in emissions which might be necessary to achieve air quality goals. For each combination of an outcome (e.g., surface ozone) and two levers or interventions (e.g., target global mean surface temperature (T) and NO_x emissions, or SO_x emissions and ammonia emissions), a separate surface is fitted in each location, ensuring that location-specific chemical regimes and responses are captured.

2.1. Atmospheric Modeling

We calculate surface air quality for a given combination of climate scenario and emission perturbation using two linked models: the Community Atmosphere Model (CAM) v3.1 and a version of the GEOS-Chem High Performance (GCHP) regional-to-global air quality model which we modify to use meteorology generated by CAM.

Meteorological data for each climate projection are generated using CAM v3.1 as detailed by Monier et al.,[29] following scenarios "POL3.7" (3.7 W/m^2 in 2100, resulting in 1.1 °C of warming in 2080−2100 relative to the 1990−2009 period) and "REF" (10 W/m^2, 4.3 °C of warming) as described therein. This framework was evaluated in Monier et al.[30] and found to produce a realistic simulation of observed climate trends. We use an ensemble approach, performing five different realizations using different sea surface wind stresses. Simulations are performed in CAM v3.1 at a global resolution of 2° × 2.5° on 26 vertical levels from the surface to a pressure of 2.2 hPa. To enable the use of this meteorology in GEOS-Chem, the same key variables are stored as are available from the NASA GMAO Modern Era Retrospective for Research and Analysis version 2 (MERRA-2) reanalysis data set and at the same temporal resolution. As a result, GCHP can be seamlessly switched between using meteorological data from MERRA-2 and from CAM.

Once meteorological data are available from CAM for each scenario realization, they are processed for use in GCHP. This approach means that emissions and meteorology can be decoupled in GCHP, allowing climate-focused and air quality-focused interventions to be assessed as separate levers. It also avoids chaotic chemistry-climate feedbacks that would otherwise take decades to average out but that do not fundamentally change the nature of the response. Surface-level concentrations of CO_2 are prescribed in GCHP based on the appropriate climate projection. CO_2 is assumed to be uniformly distributed, while the distribution of surface methane concentrations is simulated by scaling observations from NOAA (spatially kriged) to provide the correct annual mean surface concentration.[31]

Global, anthropogenic emissions of all non-greenhouse gas (non-GHG) species are prescribed based on the estimate for 2014 from the Community Emissions Data Set (CEDS).[32] Surface-level concentrations of long-lived species (other than CO_2) in GCHP are also prescribed for 2014 using existing emission inventories. Emissions of biogenic species, soil NO_x, and sea salt are estimated during the simulation based on meteorological conditions for the given scenario and, in the case of biogenic emissions, on the scenario-specific CO_2 concentration. Emissions of lightning NO_x and mineral dust are prescribed based on a 2014 inventory for all simulation years.

Since GCHP is using a new source of meteorological data, we evaluate the skill of the model by comparing observed concentrations of surface ozone to that simulated using both the "standard" configuration and the new meteorology. Figure S2 compares annual mean surface ozone between observational data (2010−2014, inclusive) from the TOAR-I data set[33,34] (https://igacproject.org/activities/TOAR) and values simulated using GCHP for 2014. We evaluate both the performance of a standard configuration of GCHP using meteorological data from the NASA Global Modeling and Assimilation Office the Modern Era Retrospective for Research and Analysis version 2 (GMAO MERRA-2) reanalysis and using data from CAM. The MERRA-2 data set was generated using the Goddard Earth Observation System (GEOS) model and is one of two GEOS output data sets which are routinely used in assessments of air quality.[35−38]

Considering the agreement between observed ozone and that simulated using MERRA-2 input (Figure S2, left panel), we find an r^2 of 0.23, a slope of 0.58, and a mean bias of 7.9 ppbv. The simulation using CAM data has an r^2 of 0.29, a slope of 0.73, and a mean bias of 15 ppbv, indicating a greater ability to represent differences between regions but a larger absolute error. Both simulations use identical emission data. On the basis of these results, we conclude that the model skill is not significantly degraded by the use of CAM meteorology compared to the use of GEOS meteorology. Parity plots, an evaluation of seasonal changes in model skill, the methods used to process the TOAR-I data, and an evaluation of model skill for wet deposition of sulfur and nitrogen are provided in the Supporting Information.

2.2. Fitting a Response Surface

For each location, we characterize the mathematical relationship between interventions (i.e., policy) and outcomes using data from the aforementioned CAM−GCHP simulations. Consider an environmental outcome that decision makers seek to achieve, such as a

https://doi.org/10.1021/acsenvironau.2c00054
ACS Environ. Au 2023, 3, 153−163

reduction in the ozone level in a single location. Any such quantity can be described as a function of factors typically related to climate change, factors typically related to air quality, and inherent uncertainty (chaos). The former factors include the total emissions of CO_2, N_2O, and CH_4 to date and the subsequent changes in the global climate. "Air quality-relevant" factors include the local emissions of nitrogen oxides (NO_x), sulfur oxides (SO_x), and ammonia (NH_3) as well as the emissions in other locations around the globe. The remaining factor is the chaotic nature of the atmosphere, resulting in uncertainty—typically expressed as a dependency on an initial condition. The model can therefore be expressed as

$$X = f(\mathbf{C}_{i=1-N}, \mathbf{S}_{j=1-M}, U)$$

where X is the objective quantity in some single location, $\mathbf{C}$ is a vector of N "climate-related" factors, $\mathbf{S}$ is a vector of M shorter-term "air quality-related" factors, and U is a variable representing the initial conditions. Members of each vector can reflect any input variable—including different species being emitted, different sectors or geographical source locations, or different times of the emission.

For many outcomes of climate change, vector $\mathbf{C}$ might be approximated with a single scalar value. Since climate change is a global phenomenon with little sensitivity to the location of the cause (e.g., the location of CO_2 emissions), its effect in any given location can mostly be captured through a scalar such as the mean CO_2 equivalent mixing ratio, global radiative forcing, or global mean surface temperature. This reduces the model to

$$X = f(R, \mathbf{S}_{j=1-M}, U)$$

where vector $\mathbf{C}$ is now replaced with scalar R. The left panel of Figure 1 illustrates how a conventional air quality study might then evaluate the effect of climate change on surface air quality through four simulations, where each simulation provides an estimate of X under different conditions. In this illustrative case, U is neglected, assuming that we are considering a single "realization" of the atmosphere.

For each climate scenario, the full curve of possible results is shown, with each pair of simulations (A and B, C and D) providing the results for two scenarios along that curve. The figure also illustrates how each pair of results can be used to derive the marginal sensitivity of surface ozone to NO_x in each climate scenario (dX/dS), while pairing point A with point C and point B with point D enables calculation of the climate penalty ($f(800,S)-f(600,S)$).

The effect of climate change on air quality can also be visualized as an intervention, or lever (i.e., an independent variable), in the same fashion as NO_x emissions, allowing their combined effect to be considered. The right panel of Figure 1 instead plots these four results as point estimates of a response surface. This recognizes that the effects of both dimensions (CO_2 and NO_x) on air quality are continuous. Furthermore, we can fit a two-dimensional response surface (most simply, a plane) to the four points, in this case with a least-squares fit. This allows us to gain insight into the response of our target variable for climate scenarios other than the two explicitly assessed by assuming linearity in the response. Although this introduces error, it exploits the broadly linear behavior of the atmosphere in response to perturbations. If we use global mean surface temperature in place of CO_2 or radiative forcing, this also frames the problem in terms of a common, physical target which is robust to uncertainty in factors such as climate sensitivity.

We use this approach to generate a response surface in each model grid point with non-zero population across Earth with respect to key climate and air quality emissions, resulting in a low-cost, intermediate-fidelity global air quality model. We calculate the response of ozone and $PM_{2.5}$ concentration across the world to changes in climate (expressed as a target global mean surface temperature T) and air quality emissions (NO_x, SO_x, VOCs, and ammonia). For each outcome and combination of two input variables (e.g., T and NO_x), we fit a response surface in each location which is described by three fit parameters (baseline value and gradient with respect to each parameter), producing a global model of air quality−climate interactions which can be applied in milliseconds.

2.3. Experimental Design

Data for fitting each response surface are generated using the GCHP (Eastham et al., 2018) chemistry transport model as described in Section 2.1. We use GCHP to simulate global air quality in the 2090s with year-2014 anthropogenic emissions of NO_x, SO_x, VOCs, and ammonia. Year-2014 emission data are used to provide a known baseline distribution and magnitude of emissions, but subsequent studies might consider using projections based on plausible scenarios of future emission changes.[39] The simulation is repeated four additional times, with a 10% reduction in global emissions of each pollutant (i.e., five simulations total). This exercise is performed for two different climate projections, consistent with a 2080−2100 mean warming (relative to 1990−2009) of either 1.1 or 4.3 °C. The results of each simulated combination of surface temperature and air quality emissions are taken as the average result across all five realizations. The change in global mean surface temperature (ΔT) is used as the policy lever to represent climate change. This is consistent with its role in models such as DICE, which use global mean temperature as the key climate metric and calculate outcomes dependent on that target.

The result is a set of 10 data points describing the concentration of ozone (or $PM_{2.5}$) in each location globally under each climate projection and each air quality perturbation. For any set of two input variables (e.g., ΔT and NO_x emissions), a linear, 2-D response surface is fit to the relevant data points for each grid cell, producing a linearized model of the response of ozone (or $PM_{2.5}$) in that location to changes in both variables. If one of the two variables is ΔT, the fit is made to four points (e.g., 100% NO_x at 1.1 °C, 90% NO_x at 1.1 °C, 100% NO_x at 4.3 °C, and 90% NO_x at 4.3 °C). If both variables are air quality only, three points are used (e.g., 100% NO_x and VOCs, 100% NO_x and 90% VOCs, 90% NO_x and 100% VOCs) as combined reductions in air quality-relevant pollutants ("cross-terms") are not simulated.

All simulations are performed for the period 2079−2099, with results stored hourly. The air quality response is calculated by averaging the results from the period 2080−2099 to compensate for meteorological variability,[40] with the 1 year period 2079−2080 discarded to avoid interference from transient "spin-up" effects. Simulations are performed at a global resolution of C24, roughly equivalent to 4° × 5°. Regional variations in air quality are therefore captured in response to global changes in climate and air quality precursor emissions.

2.4. Quantifying and Visualizing the Effect of Emission Reductions

Figure 2 shows how we fit the results from the simulations described above, where a response surface has been fit to the four points for a single location. We extrapolate or interpolate in areas where we have not explicitly calculated the response, indicated by a transition from opaque/blue to transparent/red in the figure. This fit is performed independently for each populated location on Earth, resulting in 1525 independent fits of the response of ozone (or $PM_{2.5}$) to each combination of two input variables. Combined, these produce a model which can rapidly estimate the global, spatially discretized response of air quality to combined changes in radiative forcing and air quality precursor emissions.

The use of a linear approximation is common in air quality calculations, as represented through marginal sensitivities.[10,41,42] Although the climate response to small perturbations is chaotic, atmospheric chemistry is broadly linear when examined at scale or for small changes in emissions. However, large changes in either future climate or emissions may result in substantial nonlinearity which would not be captured when using a linear assumption.[43] This could be addressed by calculating additional data points and using a nonlinear fitting procedure.

https://doi.org/10.1021/acsenvironau.2c00054
ACS Environ. Au 2023, 3, 153−163

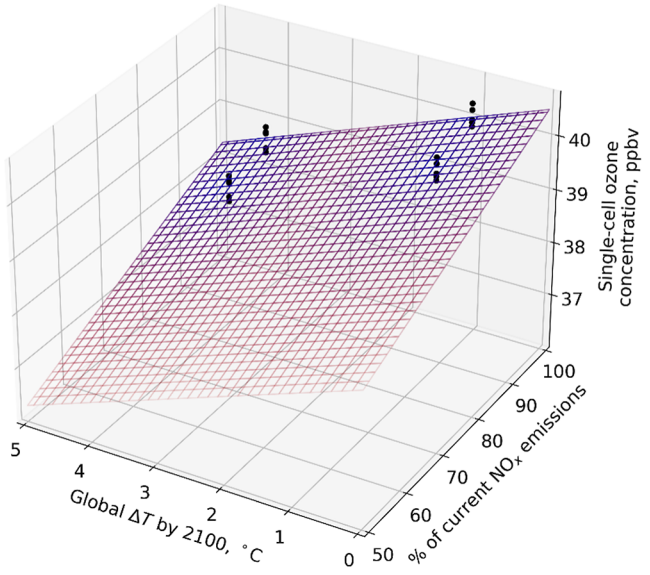

Figure 2. Demonstration of the fitting procedure. For each individual cell, we calculate the 20 year, 5-member-ensemble outcome—in this case ozone concentration—for four different scenarios (black points). A plane is then fit through these 20 points to provide a linearized estimate of the local ozone response to changes in climate (represented by the change in global surface temperature) or emissions of (e.g.) NO_x. Colors indicate qualitatively where we are performing less (blue, solid) or more (red, faded) interpolation or extrapolation.

2.5. Application in This Work

In our analysis, rather than quantifying the average surface ozone or $PM_{2.5}$ for each location under every combination of emissions, we instead quantify the fraction of a given population which would be exposed to pollution in excess of targets of either 50 ppbv maximum annual mean ozone exposure (MDA8, or maximum daily average over 8 hours) or 8 $\mu g/m^3$ annual mean $PM_{2.5}$ exposure. We refer to this quantity as the "population fraction with exposure above the target". This approach reduces the risk of a low average value hiding inequities in population exposure.

To visualize this result, we use the response surfaces calculated for each model grid cell in a single region to determine whether the population in that location will be exposed to an ozone (or $PM_{2.5}$) concentration in excess of the target for a given combination of two input variables (e.g., 10% reduction in NO_x emissions and a global mean surface temperature increase of 4.3 °C). This is summed, weighted by population, across all grid cells in a given region to determine what fraction of the region's population will be exposed to concentrations in excess of the target. By repeating this procedure while sweeping through possible combinations of input variables, an aggregate surface can be created, which shows the fraction of the region's population with exposure above the target as a function of the input variables.

Throughout this article, we show these surfaces split into three zones, depending on the degree of extrapolation underlying the result. Data shown outside of the innermost region rely on extrapolation, so although they still reflect the marginal sensitivity under different regimes, they should be interpreted with care. This is consistent with the broader approach of using marginal sensitivities to evaluate the effects of significant changes in emissions.[9,10,41,44] A description of the three zones is shown in each figure's caption.

3. RESULTS

We first use our approach to quantify the sensitivity of air quality to emissions of two short-lived pollutants under a "low-GHG" (1.1 °C of warming in 2100) future with year-2014 emissions of NO_x, VOCs, and other pollutants. Figure 3 shows how the population fraction with exposure above the surface ozone target in four different regions (global, US, China, and the EU27) varies for different levels of VOC emissions, NO_x emissions, or both. Outcomes are extrapolated to cover 0 to 50% reduction in pollutant emissions relative to 2014. The results extrapolated to 100% reductions are shown in the Supporting Information.

Aggregating globally, reductions of 50% in either NO_x or VOC emissions consistently result in a reduction in the total population fraction with exposure above the target, together reducing the fraction from 44 to 27%. However, the response in individual regions is more complex. In China, we find that the atmosphere is at least partially VOC-sensitive, such that reducing NO_x emissions by 50% without any VOC controls increases the fraction above the target from 46 to 55%. However, reducing VOC emissions alone by 50% can reduce the fraction to 29%, while combined NO_x and VOC reductions bring the fraction down to 17%. Rather than indicating a single "dominant" chemical regime, this likely reflects the heterogeneity of chemical regimes across China (see Figure S6) such that combined reductions are needed.

In the US, we find that lowering NO_x emissions by 50% reduces the fraction of the population above the target exposure from 82 to 63%, a greater benefit than when VOC emissions are reduced. This suggests NO_x-sensitive regimes across most of the US for 2014-like emissions and conditions. Again, combined reductions ensure that both NO_x- and VOC-sensitive regions are addressed, resulting in the total population fraction with exposure above our target being reduced to 56%. As in China, our result does not capture a change in chemical regime but rather reflects the fact that combined reductions in VOCs and NO_x allow ozone to be brought down regardless of the current chemical regime. Similar behavior is observed in the EU, where ozone levels are generally lower, and when aggregated globally.

Figure 4 integrates climate change as an independent variable, showing how the fraction of the population above the target exposure level changes in response to reduced global warming and NO_x emissions in 2100. Outcomes are extrapolated to cover the range of 0 to 5 °C of global mean surface temperature change. Globally, we find a near-linear relationship between each independent variable and the population fraction with exposure greater than the given ozone target. Reducing the year-2080−2100 warming from 5 to 0 °C reduces the fraction from 46 to 44%. Reducing NO_x emissions to 50% while remaining at 5 °C has a similar effect, dropping the fraction again to 44%. Combined reductions in warming and NO_x emissions yield an additional nonlinear benefit, reducing the fraction to 35%. Similarly, reductions in either warming or NO_x emissions cause monotonic decreases in the population fraction above the target exposure for the EU27 region.

This monotonic improvement is not observed in all regions. For the US, reducing warming without any reduction in NO_x emissions results in a small increase in the population fraction above the target exposure, from 80 to 83%. This behavior reverses as NO_x emissions are reduced, and for 50% NO_x emissions, we find that reducing warming from 5 to 0 °C reduces the fraction from 67 to 63%. In China, reducing warming always results in a reduction in the fraction exposed to excessive ozone. However, reducing NO_x emissions without addressing warming causes the fraction exposed to increase

https://doi.org/10.1021/acsenvironau.2c00054
ACS Environ. Au 2023, 3, 153−163

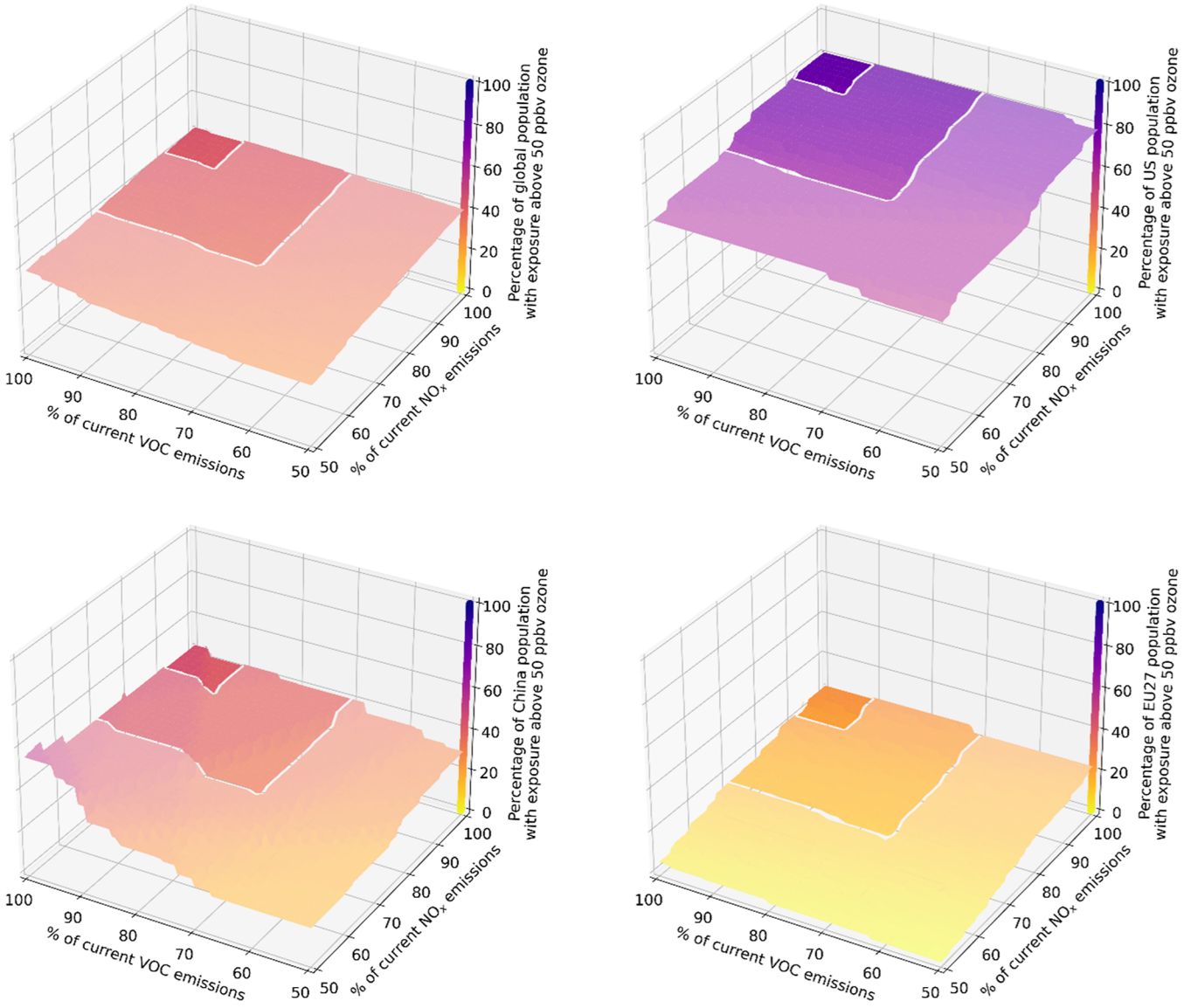

Figure 3. Response of surface ozone in 2080−2100 to reductions in VOC (x-axis) and NO_x emissions (y-axis). The results are shown in terms of the percentage of the target region population for whom exposure is above 50 ppbv. Different panels show different regions, indicated on the vertical (z) axis. The results are shown for a 2080−2100 warming of 1.1 °C. Shading indicates the value on the vertical axis, as indicated by the color bar. The darkest region indicates the results which are interpolations of simulations only, the adjacent region shows extrapolations to less than three times the base range, and the lightest region shows extrapolations beyond three times.

from 50 to 83%, highlighting the importance of considering changes in baseline exposure and not just in the marginal sensitivity to emissions. This behavior does not strongly emerge within the range of points which are interpolated between the four explicitly simulated conditions (the darkest region shown), and thus, additional simulations to directly explore the effect of larger reductions are needed to add confidence to this result.

Figure 5 shows the response of anthropogenic $PM_{2.5}$ to warming and ammonia (NH_3) emissions in the same four regions. The results for China and globally show almost no sensitivity to temperature and ammonia. In the US and EU27 however, reducing ammonia emissions yields monotonically increasing reductions in the fraction of the population with exposure above the target. At high warming levels (5 °C), 11% of the US and 4.8% of the EU27 region populations are brought from above the target exposure to below it when ammonia emissions are reduced by 50%. However, in the EU27 region, a 5 °C reduction in the target surface temperature decreases this sensitivity to a 2.8% change. In China, the fraction above the target exposure remains at between 99 and 100% regardless of target surface temperature or NH_3 emission level. Globally, 82% of the population have exposure greater than the target when ammonia emissions are reduced, compared to 85% for no reduction. The fraction is relatively insensitive to temperature, falling from 85 to 84% as the target surface temperature change is reduced from 5 to 0 °C.

4. DISCUSSION AND CONCLUSIONS

Our results for the sensitivity of air quality to reductions in NO_x and VOCs alone are consistent with the current literature, indicating that the underlying model structure is appropriate for air quality assessments. Our analysis of the air quality

https://doi.org/10.1021/acsenvironau.2c00054
ACS Environ. Au 2023, 3, 153−163

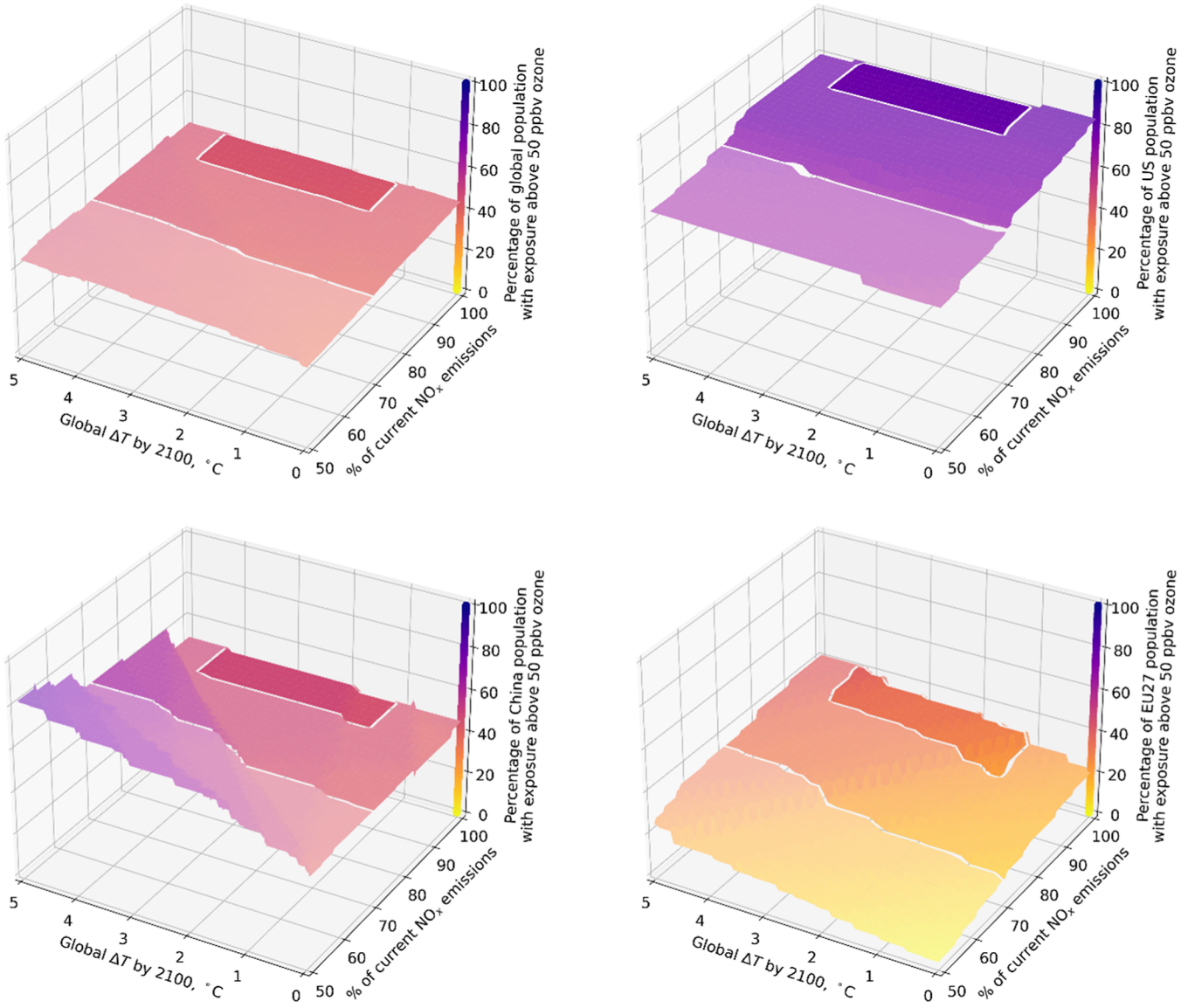

Figure 4. Response of surface ozone in 2080−2100 to reductions in future global mean surface temperature (x-axis) and NO_x emissions (y-axis). The results are shown in terms of the percentage of the target region population for whom exposure is above 50 ppbv. Different panels show different regions. Shading indicates the value on the vertical axis, as indicated by the color bar. The darkest region indicates the results which are interpolations of simulations only, the adjacent region shows extrapolations to less than three times the base range, and the lightest regions shows extrapolations beyond three times.

response to NO_x and VOCs in China in a scenario with low-background GHGs and near-current day pollutant emissions indicates the influence of a mix of NO_x-sensitive and VOC-sensitive regions. This is consistent with a recent study which found that NO_x controls in China have been ineffective in controlling urban ozone pollution.[45] Meanwhile, the simulated response of US air quality to NO_x and VOCs shows NO_x-sensitive conditions with relatively little sensitivity to VOCs. This is consistent with observed changes in the US chemical regime which are likely due to falling NO_x emissions and the relatively high concentration of biogenic VOCs.[46−48]

Using a spatially disaggregated approach allows for different chemical regimes in one region to be captured in a rapid assessment model. In China, for example, we find a greater benefit for combined reduction of NO_x and VOCs compared to the sum of benefits from reducing each independently. This indicates the existence of a mix of VOC-sensitive and NO_x-sensitive regions, which could not be captured by approaches which treat the region and its air quality monolithically. The ability to represent spatial heterogeneity allows us to provide information on how to achieve benefits (or mitigate damages) for the largest possible population. With additional simulations, our approach could also indicate changes in the chemical regime which might occur at lower emission levels.

These results indicate that our approach, despite being produced with a relatively coarse global model, is able to capture heterogeneity in the response of air quality to changes in emissions. Our method constitutes a reduced order approach to evaluate interactions between climate and air quality policy in terms of their impacts on public health. We assume linearity in the response of air quality to climate and air quality policy and neglect interactions between pollutants in individual locations. However, by developing an independent fit of the response in every grid cell, our metric incorporates

https://doi.org/10.1021/acsenvironau.2c00054
ACS Environ. Au 2023, 3, 153−163

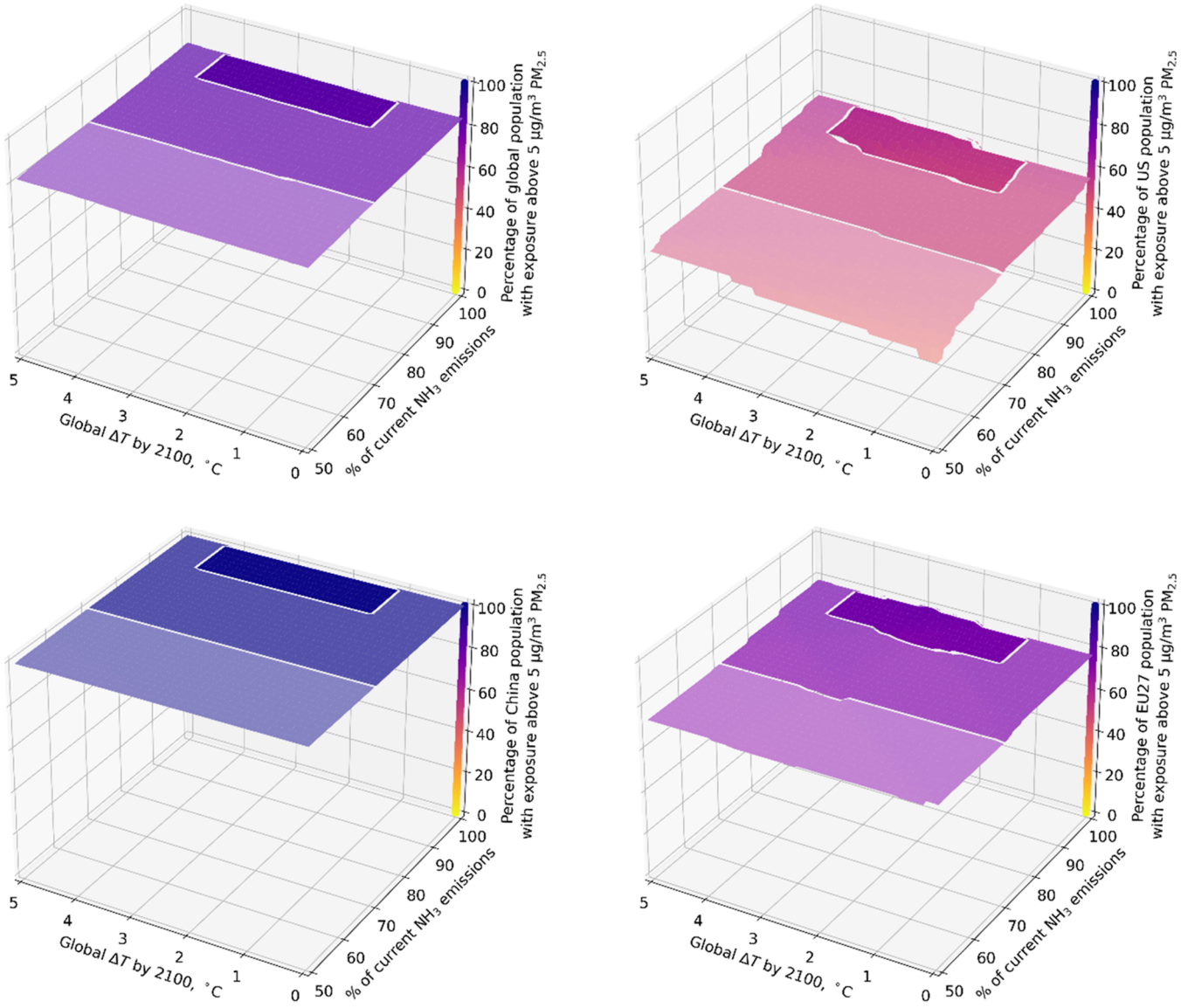

Figure 5. Response of surface anthropogenic $PM_{2.5}$ in 2080−2100 to reductions in future global mean surface temperature (x-axis) and NH_3 emissions (y-axis). The results are shown in terms of the percentage of the target region population for whom exposure is above 5 $\mu g/m^3$. Different panels show different regions. Shading indicates the value on the vertical axis, as indicated by the color bar. The darkest region indicates the results which are interpolations of simulations only, the adjacent region shows extrapolations to less than three times the base range, and the lightest region shows extrapolations beyond three times.

information on the differing chemical regimes across different locations. The results from work following this approach can be easily incorporated into IAMs by providing three fit parameters for each location and outcome (ozone and $PM_{2.5}$), thereby advancing the ability of those models to represent the effects of both climate and air quality policy on air quality outcomes. Future work using higher-resolution modeling is expected to provide more granular information regarding the response of individual locations.

Differing sensitivities in different regions demonstrate the limitations of a co-benefits framing for climate−air quality interactions. Although reductions in global warming are effective in improving air quality in many locations and sometimes yield compounding benefits, our results show that the air quality co-benefit of climate policy is dependent on air quality precursor emission stringency. The level of air quality benefit resulting from climate policy (reduced surface temperature change) relative to the benefit from air quality policy (reduced air quality precursor emissions) varies significantly by region, indicating that different regions will rationally prioritize different balances between climate and air quality policy. For example, we show NO_x reductions to be effective at reducing ozone in the EU27 under all warming scenarios, whereas they vary from ineffective to potentially harmful in China depending on the degree of warming. We also show that the effectiveness of ammonia controls in reducing exposure to $PM_{2.5}$ found in studies focusing on current conditions[49] may be affected by climate change. These differences are likely due to the effect of climate change on meteorology, including the effect of changes in specific humidity and precipitation. We also find that an air quality "co-benefit" of avoiding climate change is not inevitable, such as the increase in the fraction of the EU population exposed to high levels of $PM_{2.5}$ with decreasing surface temperature. Our results support the need for holistic

https://doi.org/10.1021/acsenvironau.2c00054
ACS Environ. Au 2023, 3, 153−163

assessments of climate and air quality policy, and our approach provides a methodology to perform such assessments.

In summary, this new approach enables rapid assessment modeling for air quality−climate interactions. We provided spatially disaggregated ozone and $PM_{2.5}$ estimates, splitting the global response into 1525 independent subregions. For each region, we estimated the air quality response to policy which affects global surface temperature, air quality precursor emissions, or both. This enabled a first-order assessment of how climate and air quality policy might affect both the magnitude and distribution of air quality degradation worldwide within milliseconds, bridging the gap between integrated assessment modeling and high-fidelity chemistry-climate simulation.

The results shown here can be adapted to address several urgent, pertinent questions in the realm of climate and air quality interactions. This approach could be applied to estimate the integrated air quality impacts of any combined climate−air quality policy scenario on air quality outcomes, allowing decision makers to understand how air quality policy will be affected by a warming climate. This could include both evaluation of impacts and the identification of new policy options. Since the results of the approach are not tied to specific air quality or climate scenarios, a broader range of outcomes can be investigated than is possible with traditional single-scenario assessments.

There are several avenues to improve or extend our approach without increasing the number of simulations required. The use of a higher-resolution model would capture more granularity in the impacts on specific demographics and better capture heterogeneity in chemical regimes. This would increase the computational cost required to generate the original response surfaces but would not significantly increase the cost of using the surfaces in an IAM context. This is because, once the initial fit parameters have been generated, a global evaluation currently requires less than 1 second to perform on a single processor. If the focus is on large reductions, it may be preferable to fit the response surface based on reductions in emissions which are greater than 10%, although this would then reduce the accuracy for smaller changes.

More generally, our method could be extended by performing additional simulations to develop a more complex response surface, effectively increasing the number of arguments considered in its functional form. The climate-relevant factors could be separated so that surface warming and background methane concentrations are decoupled, rather than ignored or rather simplistically treated as a single coupled parameter. Simulations with a simultaneous reduction in multiple variables could be used to determine "cross-terms" (e.g., with simultaneous reductions in VOCs and NO_x) or to explore further out in the parameter space and add confidence in findings which are currently the result of extrapolation (e.g., simulate 50 or 100% reduction in NO_x). A more complex paraboloid fit to these points in each location would allow changes in chemical regime to be captured. Finally, we consider only global changes in air quality emissions. Emissions scaling by location and/or by sector could enable evaluation of the impact of more targeted air quality policy under an uncertain climate future.

This approach can also be further extended beyond air quality outcomes. Although the data shown in this article focus on interactions between climate policy (future global mean surface temperature) and air quality policy (emissions of NO_x, VOCs, and so on), our approach could equally be applied to investigate interacting air pollutants or any other environmental policy question.

■ ASSOCIATED CONTENT

Data Availability Statement

The GCHP model code used in this study is available at https://doi.org/10.5281/zenodo.7612758. A sample simulation directory is available at https://doi.org/10.5281/zenodo.7618576. A condensed set of output files is available at https://doi.org/10.5281/zenodo.7618605, and a sample analysis code which demonstrates the emulation (reproducing two of this paper's key figures) is available at https://doi.org/10.5281/zenodo.7618827. The ensemble of meteorological input data are available from the authors upon request for those wishing to run GCHP directly with CAM input. These data are not required to use the emulation approach described in this paper.

Supporting Information

The Supporting Information is available free of charge at https://pubs.acs.org/doi/10.1021/acsenvironau.2c00054.

Evaluation of present-day performance of the GCHP−CAM system against observations; estimate of global NO_x sensitivity; and extended/extrapolated versions of Figures 3−5 (PDF)

■ AUTHOR INFORMATION

Corresponding Author

Sebastian D. Eastham − *Laboratory for Aviation and the Environment, Massachusetts Institute of Technology, Cambridge, Massachusetts 02139, United States; Joint Program on the Science and Policy of Global Change, Massachusetts Institute of Technology, Cambridge, Massachusetts 02139, United States;* orcid.org/0000-0002-2476-4801; Email: seastham@mit.edu

Authors

Erwan Monier − *Joint Program on the Science and Policy of Global Change, Massachusetts Institute of Technology, Cambridge, Massachusetts 02139, United States; Land, Air and Water Resources, University of California Davis, Davis, California 95616, United States*

Daniel Rothenberg − *Joint Program on the Science and Policy of Global Change, Massachusetts Institute of Technology, Cambridge, Massachusetts 02139, United States*

Sergey Paltsev − *Joint Program on the Science and Policy of Global Change, Massachusetts Institute of Technology, Cambridge, Massachusetts 02139, United States*

Noelle E. Selin − *Institute for Data, Systems, and Society and Department of Earth, Atmospheric, and Planetary Sciences, Massachusetts Institute of Technology, Cambridge, Massachusetts 02139, United States;* orcid.org/0000-0002-6396-5622

Complete contact information is available at: https://pubs.acs.org/10.1021/acsenvironau.2c00054

Author Contributions

N.E.S. conceived of the study and provided oversight. Development of the GCHP−CAM interface was performed by S.D.E. with assistance from D.R. and E.M. E.M. performed

https://doi.org/10.1021/acsenvironau.2c00054
ACS Environ. Au 2023, 3, 153−163

the CAM simulations. S.D.E. performed GCHP simulations and analysis. S.P. provided EPPA input and developed the emission matching scheme. S.D.E. and N.E.S. produced the first draft of the manuscript collaboratively. All authors took part in manuscript edits and revisions. CRediT: **Sebastian D. Eastham** conceptualization (supporting), formal analysis (equal), investigation (equal), methodology (lead), software (lead), validation (equal), visualization (equal), writing-original draft (lead), writing-review & editing (equal); **Erwan Monier** methodology (equal), software (supporting), writing-review & editing (equal); **Daniel Rothenberg** conceptualization (equal), methodology (equal), software (supporting), writing-review & editing (equal); **Sergey Paltsev** formal analysis (supporting), methodology (supporting), software (supporting), writing-review & editing (equal); **Noelle E Selin** conceptualization (lead), formal analysis (equal), funding acquisition (lead), project administration (equal), resources (lead), supervision (lead), visualization (supporting), writing-original draft (equal), writing-review & editing (equal).

Notes

The authors declare no competing financial interest.

■ ACKNOWLEDGMENTS

The MERRA-2 data used in this study/project have been provided by the Global Modeling and Assimilation Office (GMAO) at NASA Goddard Space Flight Center. Ozone observation data were acquired from the first phase of the Tropospheric Ozone Assessment Report (TOAR) initiative (http://www.igacproject.org/activities/TOAR). This publication was partially supported by the US EPA (grant no. RD-835872-01). Its contents are solely the responsibility of the grantee and do not necessarily represent the official views of the US EPA. Further, the US EPA does not endorse the purchase of any commercial products or services mentioned in the publication. This study was also supported by Biogen Inc.

■ REFERENCES

(1) Fiore, A. M.; Naik, V.; Leibensperger, E. M. Air Quality and Climate Connections. *J. Air Waste Manag. Assoc.* **2015**, *65*, 645−685.
(2) Fu, T.-M.; Tian, H. Climate Change Penalty to Ozone Air Quality: Review of Current Understandings and Knowledge Gaps. *Curr. Pollut. Rep.* **2019**, *5*, 159−171.
(3) Garcia-Menendez, F.; Monier, E.; Selin, N. E. The role of natural variability in projections of climate change impacts on U.S. ozone pollution. *Geophys. Res. Lett.* **2017**, *44*, 2911−2921.
(4) Garcia-Menendez, F.; Saari, R. K.; Monier, E.; Selin, N. E. U. S. U.S. Air Quality and Health Benefits from Avoided Climate Change under Greenhouse Gas Mitigation. *Environ. Sci. Technol.* **2015**, *49*, 7580−7588.
(5) Hegwood, M.; Langendorf, R. E.; Burgess, M. G. Why Win−Wins Are Rare in Complex Environmental Management. *Nat. Sustain.* **2022**, *5*, 674−680.
(6) Reis, A. L.; Drouet, L.; Dingenen, R.; Emmerling, J. Future Global Air Quality Indices under Different Socioeconomic and Climate Assumptions. *Sustain. Sci. Pract. Pol.* **2018**, *10*, 3645.
(7) Rao, S.; Klimont, Z.; Smith, S. J.; Van Dingenen, R.; Dentener, F.; Bouwman, L.; Riahi, K.; Amann, M.; Bodirsky, B. L.; van Vuuren, D. P.; Aleluia Reis, L.; Calvin, K.; Drouet, L.; Fricko, O.; Fujimori, S.; Gernaat, D.; Havlik, P.; Harmsen, M.; Hasegawa, T.; Heyes, C.; Hilaire, J.; Luderer, G.; Masui, T.; Stehfest, E.; Strefler, J.; van der Sluis, S.; Tavoni, M. Future Air Pollution in the Shared Socio-Economic Pathways. *Global Environ. Change* **2017**, *42*, 346−358.
(8) Buonocore, J. J.; Dong, X.; Spengler, J. D.; Fu, J. S.; Levy, J. I. Using the Community Multiscale Air Quality (CMAQ) model to estimate public health impacts of PM2.5 from individual power plants. *Environ. Int.* **2014**, *68*, 200−208.
(9) Barrett, S. R. H.; Speth, R. L.; Eastham, S. D.; Dedoussi, I. C.; Ashok, A.; Malina, R.; Keith, D. W. Impact of the Volkswagen Emissions Control Defeat Device on US Public Health. *Environ. Res. Lett.* **2015**, *10*, 114005.
(10) Dedoussi, I. R.; Eastham, S. D.; Monier, E.; Barrett, S. R. H. Premature Mortality Related to United States Cross-State Air Pollution. *Nature* **2020**, *578*, 261−265.
(11) Sofiev, M.; Winebrake, J. J.; Johansson, L.; Carr, E. W.; Prank, M.; Soares, J.; Vira, J.; Kouznetsov, R.; Jalkanen, J.-P.; Corbett, J. Cleaner fuels for ships provide public health benefits with climate tradeoffs. *Nat. Commun.* **2018**, *9*, 406.
(12) Kinney, P. L. How Can We Solve Our Air Quality Problem in the Face of Climate Change? *JAMA Netw. Open* **2021**, *4*, No. e2035010.
(13) Kinney, P. L. Interactions of Climate Change, Air Pollution, and Human Health. *Curr. Environ. Health Rep.* **2018**, *5*, 179−186.
(14) von Schneidemesser, E.; Driscoll, C.; Rieder, H. E.; Schiferl, L. D. How Will Air Quality Effects on Human Health, Crops and Ecosystems Change in the Future? *Philos. Trans. R. Soc., A* **2020**, *378*, 20190330.
(15) Westervelt, D. M.; Ma, C. T.; He, M. Z.; Fiore, A. M.; Kinney, P. L.; Kioumourtzoglou, M.-A.; Wang, S.; Xing, J.; Ding, D.; Correa, G. Mid-21st Century Ozone Air Quality and Health Burden in China under Emissions Scenarios and Climate Change. *Environ. Res. Lett.* **2019**, *14*, 074030.
(16) Nguyen, G. T. H.; Shimadera, H.; Uranishi, K.; Matsuo, T.; Kondo, A. Numerical Assessment of PM_2.5 and O_3 Air Quality in Continental Southeast Asia: Impacts of Future Projected Anthropogenic Emission Change and Its Impacts in Combination with Potential Future Climate Change Impacts. *Atmos. Environ.* **2020**, *226*, 117398.
(17) Pommier, M.; Fagerli, H.; Gauss, M.; Simpson, D.; Sharma, S.; Sinha, V.; Ghude, S. D.; Landgren, O.; Nyiri, A.; Wind, P. Impact of Regional Climate Change and Future Emission Scenarios on Surface O_3 and $PM_{2.5}$ over India. *Atmos. Chem. Phys.* **2018**, *18*, 103−127.
(18) Nolte, C. G.; Spero, T. L.; Bowden, J. H.; Mallard, M. S.; Dolwick, P. D. The Potential Effects of Climate Change on Air Quality across the Conterminous US at 2030 under Three Representative Concentration Pathways. *Atmos. Chem. Phys.* **2018**, *18*, 15471−15489.
(19) Bosetti, V.; Carraro, C.; Galeotti, M.; Massetti, E.; Tavoni, M. WITCH A World Induced Technical Change Hybrid Model. *SSRN Electron. J.* **2006**, *27*, 31.
(20) Emmerling, J.; Drouet, L.; Wijst, K.-I.; Vuuren, D.; Bosetti, V.; Tavoni, M. The Role of the Discount Rate for Emission Pathways and Negative Emissions. *Environ. Res. Lett.* **2019**, *14*, 104008.
(21) van Soest, H. L.; van Vuuren, D. P.; Hilaire, J.; Minx, J. C.; Harmsen, M. J. H. M.; Krey, V.; Popp, A.; Riahi, K.; Luderer, G. Analysing Interactions among Sustainable Development Goals with Integrated Assessment Models. *Glob. Transit.* **2019**, *1*, 210−225.
(22) Nordhaus, W. Estimates of the Social Cost of Carbon: Concepts and Results from the DICE-2013R Model and Alternative Approaches. *J. Assoc. Environ. Resour. Econ.* **2014**, *1*, 273−312.
(23) Nam, K.-M.; Waugh, C. J.; Paltsev, S.; Reilly, J. M.; Karplus, V. J. Synergy between Pollution and Carbon Emissions Control: Comparing China and the United States. *Energy Econ.* **2014**, *46*, 186−201.
(24) Reis, L. A.; Drouet, L.; Tavoni, M. Internalising Health-Economic Impacts of Air Pollution into Climate Policy: A Global Modelling Study. *Lancet Planet. Health* **2022**, *6*, e40−e48.
(25) Jafino, B. A.; Hallegatte, S.; Rozenberg, J. Focusing on Differences across Scenarios Could Lead to Bad Adaptation Policy Advice. *Nat. Clim. Change* **2021**, *11*, 394−396.
(26) Jacob, D. J.; Winner, D. a. Effect of Climate Change on Air Quality. *Atmos. Environ.* **2009**, *43*, 51−63.

https://doi.org/10.1021/acsenvironau.2c00054
ACS Environ. Au 2023, 3, 153−163

(27) Heo, J.; Adams, P. J.; Gao, H. O. Reduced-Form Modeling of Public Health Impacts of Inorganic PM2.5 and Precursor Emissions. *Atmos. Environ.* **2016**, *137*, 80−89.
(28) Paltsev, S.; Monier, E.; Scott, J.; Sokolov, A.; Reilly, J. Integrated Economic and Climate Projections for Impact Assessment. *Clim. Change* **2015**, *131*, 21−33.
(29) Monier, E.; Gao, X.; Scott, J. R.; Sokolov, A. P.; Schlosser, C. A. A Framework for Modeling Uncertainty in Regional Climate Change. *Clim. Change* **2015**, *131*, 51−66.
(30) Monier, E.; Scott, J. R.; Sokolov, A. P.; Forest, C. E.; Schlosser, C. A. An Integrated Assessment Modeling Framework for Uncertainty Studies in Global and Regional Climate Change: The MIT IGSM-CAM (Version 1.0). *Geosci. Model Dev.* **2013**, *6*, 2063−2085.
(31) Murray, L. T. Lightning NO_x and Impacts on Air Quality. *Curr. Pollut. Rep.* **2016**, *2*, 115−133.
(32) Hoesly, R. M.; Smith, S. J.; Feng, L.; Klimont, Z.; Janssens-Maenhout, G.; Pitkanen, T.; Seibert, J. J.; Vu, L.; Andres, R. J.; Bolt, R. M.; Bond, T. C.; Dawidowski, L.; Kholod, N.; Kurokawa, J.-I.; Li, M.; Liu, L.; Lu, Z.; Moura, M. C. P.; O'Rourke, P. R.; Zhang, Q. Historical (1750-2014) anthropogenic emissions of reactive gases and aerosols from the Community Emissions Data System (CEDS). *Geosci. Model Dev.* **2018**, *11*, 369−408.
(33) Schultz, M. G.; Schröder, S.; Lyapina, O.; Cooper, O.; Galbally, I.; Petropavlovskikh, I.; Von Schneidemesser, E.; Tanimoto, H.; Elshorbany, Y.; Naja, M.; Seguel, R.; Dauert, U.; Eckhardt, P.; Feigenspahn, S.; Fiebig, M.; Hjellbrekke, A.-G.; Hong, Y.-D.; Christian Kjeld, P.; Koide, H.; Lear, G.; Tarasick, D.; Ueno, M.; Wallasch, M.; Baumgardner, D.; Chuang, M.-T.; Gillett, R.; Lee, M.; Molloy, S.; Moolla, R.; Wang, T.; Sharps, K.; Adame, J. A.; Ancellet, G.; Apadula, F.; Artaxo, P.; Barlasina, M.; Bogucka, M.; Bonasoni, P.; Chang, L.; Colomb, A.; Cuevas, E.; Cupeiro, M.; Degorska, A.; Ding, A.; Fröhlich, M.; Frolova, M.; Gadhavi, H.; Gheusi, F.; Gilge, S.; Gonzalez, M. Y.; Gros, V.; Hamad, S. H.; Helmig, D.; Henriques, D.; Hermansen, O.; Holla, R.; Huber, J.; Im, U.; Jaffe, D. A.; Komala, N.; Kubistin, D.; Lam, K.-S.; Laurila, T.; Lee, H.; Levy, I.; Mazzoleni, C.; Mazzoleni, L.; McClure-Begley, A.; Mohamad, M.; Murovic, M.; Navarro-Comas, M.; Nicodim, F.; Parrish, D.; Read, K. A.; Reid, N.; Ries, L.; Saxena, P.; Schwab, J. J.; Scorgie, Y.; Senik, I.; Simmonds, P.; Sinha, V.; Skorokhod, A.; Spain, G.; Spangl, W.; Spoor, R.; Springston, S. R.; Steer, K.; Steinbacher, M.; Suharguniyawan, E.; Torre, P.; Trickl, T.; Weili, L.; Weller, R.; Xu, X.; Xue, L.; Zhiqiang, M. Tropospheric Ozone Assessment Report: Database and Metrics Data of Global Surface Ozone Observations. *Elementa* **2017**, *5*, 58.
(34) Schultz, M. G.; Schröder, S.; Lyapina, O.; Cooper, O. R.; Galbally, I.; Petropavlovskikh, I.; von Schneidemesser, E.; Tanimoto, H.; Elshorbany, Y.; Naja, M.; Seguel, R. J.; Dauert, U.; Eckhardt, P.; Feigenspan, S.; Fiebig, M.; Hjellbrekke, A.-G.; Hong, Y.-D.; Kjeld, P. C.; Koide, H.; Lear, G.; Tarasick, D.; Ueno, M.; Wallasch, M.; Baumgardner, D.; Chuang, M.-T.; Gillett, R.; Lee, M.; Molloy, S.; Moolla, R.; Wang, T.; Sharps, K.; Adame, J. A.; Ancellet, G.; Apadula, F.; Artaxo, P.; Barlasina, M. E.; Bogucka, M.; Bonasoni, P.; Chang, L.; Colomb, A.; Cuevas-Agulló, E.; Cupeiro, M.; Degorska, A.; Ding, A.; Fröhlich, M.; Frolova, M.; Gadhavi, H.; Gheusi, F.; Gilge, S.; Gonzalez, M. Y.; Gros, V.; Hamad, S. H.; Helmig, D.; Henriques, D.; Hermansen, O.; Holla, R.; Hueber, J.; Im, U.; Jaffe, D. A.; Komala, N.; Kubistin, D.; Lam, K.-S.; Laurila, T.; Lee, H.; Levy, I.; Mazzoleni, C.; Mazzoleni, L. R.; McClure-Begley, A.; Mohamad, M.; Murovec, M.; Navarro-Comas, M.; Nicodim, F.; Parrish, D.; Read, K. A.; Reid, N.; Ries, L.; Saxena, P.; Schwab, J. J.; Scorgie, Y.; Senik, I.; Simmonds, P.; Sinha, V.; Skorokhod, A. I.; Spain, G.; Spangl, W.; Spoor, R.; Springston, S. R.; Steer, K.; Steinbacher, M.; Suharguniyawan, E.; Torre, P.; Trickl, T.; Weili, L.; Weller, R.; Xu, X.; Xue, L.; Zhiqiang, M. *Tropospheric Ozone Assessment Report, Links to Global Surface Ozone Datasets*; Jülich Supercomputing Centre, 2017 (accessed August 18, 2022).
(35) Vohra, K.; Vodonos, A.; Schwartz, J.; Marais, E. A.; Sulprizio, M. P.; Mickley, L. J. Global Mortality from Outdoor Fine Particle Pollution Generated by Fossil Fuel Combustion: Results from GEOS-Chem. *Environ. Res.* **2021**, *195*, 110754.
(36) Potts, D. A.; Marais, E. A.; Boesch, H.; Pope, R. J.; Lee, J.; Drysdale, W.; Chipperfield, M. P.; Kerridge, B.; Siddans, R.; Moore, D. P.; Remedios, J. Diagnosing Air Quality Changes in the UK during the COVID-19 Lockdown Using TROPOMI and GEOS-Chem. *Environ. Res. Lett.* **2021**, *16*, 054031.
(37) David, L. M.; Ravishankara, A. R.; Brewer, J. F.; Sauvage, B.; Thouret, V.; Venkataramani, S.; Sinha, V. Tropospheric Ozone over the Indian Subcontinent from 2000 to 2015: Data Set and Simulation Using GEOS-Chem Chemical Transport Model. *Atmos. Environ.* **2019**, *219*, 117039.
(38) Li, K.; Jacob, D. J.; Liao, H.; Zhu, J.; Shah, V.; Shen, L.; Bates, K. H.; Zhang, Q.; Zhai, S. A Two-Pollutant Strategy for Improving Ozone and Particulate Air Quality in China. *Nat. Geosci.* **2019**, *12*, 906−910.
(39) Atkinson, W.; Eastham, S. D.; Chen, Y.-H. H.; Morris, J.; Paltsev, S.; Schlosser, C. A.; Selin, N. E. A Tool for Air Pollution Scenarios (TAPS v1. 0) to Enable Global, Long-Term, and Flexible Study of Climate and Air Quality Policies. *Geosci. Model Dev. Discuss.* **2022**, *15*, 7767−7789.
(40) Brown-Steiner, B.; Selin, N. E.; Prinn, R. G.; Monier, E.; Tilmes, S.; Emmons, L.; Garcia-Menendez, F. Maximizing Ozone Signals among Chemical, Meteorological, and Climatological Variability. *Atmos. Chem. Phys.* **2018**, *18*, 8373−8388.
(41) Gilmore, E. A.; Heo, J.; Muller, N. Z.; Tessum, C. W.; Hill, J. D.; Marshall, J. D.; Adams, P. J. An Inter-Comparison of the Social Costs of Air Quality from Reduced-Complexity Models. *Environ. Res. Lett.* **2019**, *14*, 074016.
(42) Tessum, C. W.; Hill, J. D.; Marshall, J. D. InM. A. P. InMAP: A model for air pollution interventions. *PLoS One* **2017**, *12*, No. e0176131.
(43) Raes, F.; Liao, H.; Chen, W.-T.; Seinfeld, J. H. Atmospheric Chemistry-Climate Feedbacks. *J. Geophys. Res.* **2010**, *115*, 1−14.
(44) Tessum, C. W.; Apte, J. S.; Goodkind, A. L.; Muller, N. Z.; Mullins, K. A.; Paolella, D. A.; Polasky, S.; Springer, N. P.; Thakrar, S. K.; Marshall, J. D.; Hill, J. D. Inequity in consumption of goods and services adds to racial-ethnic disparities in air pollution exposure. *Proc. Natl. Acad. Sci. U.S.A.* **2019**, *116*, 6001−6006.
(45) Chen, X.; Jiang, Z.; Shen, Y.; Li, R.; Fu, Y.; Liu, J.; Han, H.; Liao, H.; Cheng, X.; Jones, D. B. A.; Worden, H.; Abad, G. G. Chinese Regulations Are Working—Why Is Surface Ozone over Industrialized Areas Still High? Applying Lessons from Northeast US Air Quality Evolution. *Geophys. Res. Lett.* **2021**, *48*, No. e2021GL092816.
(46) Li, J.; Wang, Y.; Qu, H. Dependence of Summertime Surface Ozone on NO_x and VOC Emissions over the United States: Peak Time and Value. *Geophys. Res. Lett.* **2019**, *46*, 3540−3550.
(47) Jung, J.; Choi, Y.; Mousavinezhad, S.; Kang, D.; Park, J.; Pouyaei, A.; Ghahremanloo, M.; Momeni, M.; Kim, H. Changes in the Ozone Chemical Regime over the Contiguous United States Inferred by the Inversion of NOx and VOC Emissions Using Satellite Observation. *Atmos. Res.* **2022**, *270*, 1−14.
(48) Koplitz, S.; Simon, H.; Henderson, B.; Liljegren, J.; Tonnesen, G.; Whitehill, A.; Wells, B. Changes in Ozone Chemical Sensitivity in the United States from 2007 to 2016. *ACS Environ. Au* **2022**, *2*, 206−222.
(49) Gu, B.; Zhang, L.; Van Dingenen, R.; Vieno, M.; Van Grinsven, H. J.; Zhang, X.; Zhang, S.; Chen, Y.; Wang, S.; Ren, C.; Rao, S.; Holland, M.; Winiwarter, W.; Chen, D.; Xu, J.; Sutton, M. A. Abating ammonia is more cost-effective than nitrogen oxides for mitigating $PM_{2.5}$ air pollution. *Science* **2021**, *374*, 758−762.

NOTE ADDED AFTER ASAP PUBLICATION

This paper was published ASAP on February 14, 2023, with errors in the Acknowledgments and captions for Figures 3 and 5. The corrected version was reposted on March 22, 2023.

https://doi.org/10.1021/acsenvironau.2c00054
ACS Environ. Au 2023, 3, 153−163